

Seismic image regularization in the reflection angle domain

Marie L. Prucha, Robert G. Clapp, and Biondo Biondi¹

ABSTRACT

We explore the use of preconditioned inversion in the reflection angle domain rather than migration to improve imaging in complex media. We use a wave-equation method to create reflection angle domain common image gathers and we apply steering filter preconditioning to smooth along the reflection angles. This improves the common image gathers. The improved common image gathers are more continuous than common image gathers obtained by migration alone. Additionally, some multiple energy is attenuated.

INTRODUCTION

Current migration methods are done mostly in the offset domain and the shot domain, which are prone to multipathing (ten Kroode et al., 1999) in complex areas. A fairly new method that is being used to image complex areas is migration in the reflection angle domain (RAD). This can be done both by Kirchhoff methods (Xu et al., 1998) and wave-equation methods (Prucha et al., 1999). The RAD avoids the problem of multipathing, and therefore contains fewer artifacts than the more commonly used domains. Unfortunately, even with fewer multipathing artifacts, in complex areas migration may not be enough. Since we are interested in complex areas, we can reformulate our imaging problem as an inversion problem (Chemingui, 1999).

Although imaging by inversion can give better results than migration, an inversion problem can be unstable (Claerbout, 1991). A trick used to constrain inversion problems to a reasonable result is regularization (Harlan, 1986; Fomel, 1997). Theory states that for a particular point in the subsurface, the reflectivity as a function of reflection angle should vary smoothly (Richter, 1941). Therefore, the obvious choice for a regularization operator in the reflection angle domain is one that smooths along the reflection angles. To speed the convergence, we can reformulate the regularization problem as a preconditioned problem (Fomel et al., 1997). We intend to show that applying this method in the reflection angle domain will improve the common image gathers (CIGs), making the events more continuous, reducing artifacts, and attenuating multiples.

In this paper, we will first explain how to image in the reflection angle domain and how to apply regularization and preconditioning. Then we will show the results of applying regularization to a RAD inversion problem on two different synthetic datasets.

¹email: marie@sep.Stanford.EDU,bob@sep.Stanford.EDU,biondo@sep.Stanford.EDU

THEORY

Migration in the reflection angle domain

Migration in the reflection angle domain is a subsurface-oriented technique. It is most easily understood as a Kirchhoff method. For each point in the subsurface (\mathbf{x}), a ray couple can be created for a certain reflection angle (θ) and a certain dip angle (ϕ) as shown in Figure 1. To create a CIG, simply sum over all of the dip angles:

$$a(\mathbf{x}, \theta) = \int w(\phi, \theta, \mathbf{x}) d(s, r, t) d\phi \quad (1)$$

where $a(\mathbf{x}, \theta)$ is the RAD CIGs, $w(\phi, \theta, \mathbf{x})$ is an appropriate weighting function, and $d(s, r, t)$ is the data in source, receiver and time space. From this, it is clear that each event in a RAD CIG is created by one and only one ray couple. This means there is no multipathing. Therefore, we will have fewer artifacts, especially in complex areas. In this paper, we actually use a wave-

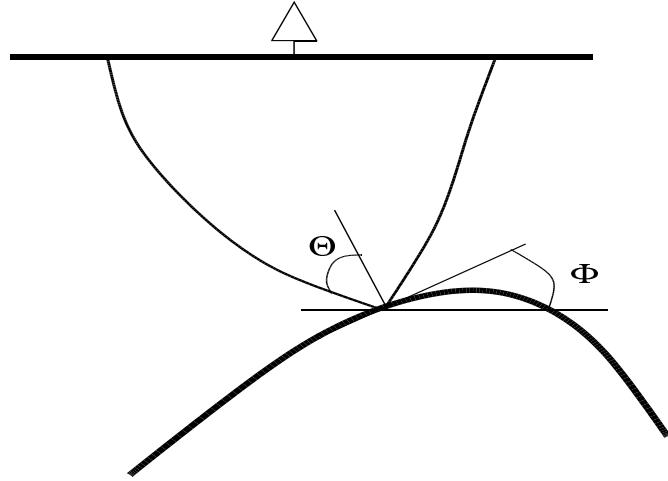


Figure 1: Geometry of the reflection angle marie1-rangle [NR]

equation method to create the RAD CIG. We begin by using the Double Square Root (DSR) equation to downward continue the data (represented as the wavefield recorded at the surface $P(\omega, \mathbf{m}, h_x; z = 0)$ where ω indicates the frequency domain, \mathbf{m} is the midpoint location, h_x is offset, and z is depth), then we slant stack (transforming the data into vertical travelttime space τ) at each depth level and image at zero time:

$$P(\omega, \mathbf{m}, h_x; z = 0) \xrightarrow{\text{DSR}} P(\omega, \mathbf{m}, h_x; z) \quad (2)$$

$$P(\omega, \mathbf{m}, h_x; z) \xrightarrow{\text{Slant stack}} P(\tau, \mathbf{m}, p_{hx}; z) \quad (3)$$

$$P(\tau, \mathbf{m}, p_{hx}; z) \xrightarrow{\text{Imaging}} P(\tau = 0, \mathbf{m}, p_{hx}; z). \quad (4)$$

The actual CIG is extracted at a fixed midpoint. The resulting CIG has an axis that is in offset ray parameter (p_{hx}) rather than reflection angle (θ). However, the offset ray parameter is related to the reflection angle by:

$$\frac{\partial t}{\partial h} = p_{hx} = \frac{2 \sin \theta \cos \phi}{V(z, \mathbf{m})}. \quad (5)$$

Sava and Fomel (2000) describe an alternative method of obtaining RAD CIGs in the Fourier domain.

The advantages of the RAD in helping to reduce illumination problems are not immediately obvious. Imagine upward continuing a wavefield from a reflector below a complex structure such as a salt dome. As the wavefield passes through the complex structure, the energy gets spread out unevenly over a large distance. In the offset and shot domains, this distribution can lead to the loss of energy that is present but doesn't conform to the regular surface-oriented geometry. The subsurface-oriented reflection angle domain does not have this difficulty. Unfortunately, there is another problem. Our acquisition geometry is always finite, therefore we can never record the entire wavefield at the surface. When we downward continue the finite recorded wavefield, the "missing" data creates a model null space. This null space cannot be filled with migration alone, so we turn to inversion.

Inversion in the reflection angle domain

Since we are using this method to image complex areas, just performing migration is not enough (Prucha et al., 1999). We want to formulate the process as an inversion problem (Nemeth et al., 1999; Duquet and Marfurt, 1999). Unfortunately, the complexity can cause the result of the inversion to diverge. Therefore, to constrain the inversion to a reasonable result, we choose to impose regularization. This can be represented by these fitting goals:

$$\mathbf{d} \approx \mathbf{Lm} \quad (6)$$

$$0 \approx \epsilon \mathbf{Am} \quad (7)$$

where \mathbf{d} is the data space, \mathbf{m} is the model space, \mathbf{L} is the wave-equation operator, \mathbf{A} is the regularization operator, and choosing the parameter ϵ is a Lagrange multiplier that allows us to determine how strong our regularization (smoothing) will be.

To speed the convergence of the inversion, we can reformulate the inversion problem as a preconditioning problem with a preconditioning operator \mathbf{S} . This operator should be as close to the inverse of the regularization operator as possible so that $\mathbf{AS} \approx \mathbf{I}$. By mapping the multi-dimensional regularization operator \mathbf{A} to helical space and applying polynomial division, we can obtain the exact inverse so that $\mathbf{S} = \mathbf{A}^{-1}$ (Claerbout, 1998). We also use the preconditioning transformation $\mathbf{m} = \mathbf{Sp}$ (Fomel et al., 1997). Our equations then become:

$$\mathbf{d} \approx \mathbf{LSp} \quad (8)$$

$$0 \approx \epsilon \mathbf{p}. \quad (9)$$

The regularization we choose for RAD inversion is horizontal smoothing along the reflection angle (or p_{hx}) axis. This is based on both theory and practice. In theory, the regularization operator should be related to the inverse model covariance matrix (Tarantola, 1986). In practice, because the covariance matrix of a CIG created with the correct velocity model is horizontal in nature (Figure 2) and the reflectivity along reflection angles should vary smoothly (Richter, 1941), we simply smooth horizontally along the reflection angle axis. An operator that fulfills these requirements is a steering filter (Clapp et al., 1997). This steering filter and its impulse

response is in Figure 3. The coefficients in the second column of the steering filter are variable and control the vertical width of the impulse response.

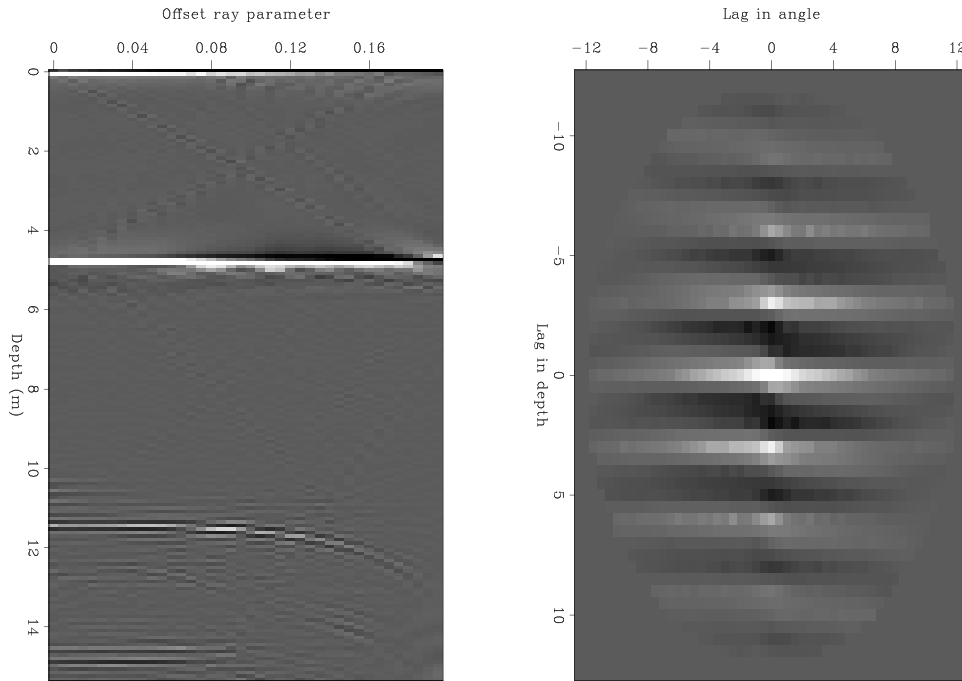


Figure 2: Left: a typical RAD CIG with some minor artifacts. Right: representation of the covariance matrix calculated for this CIG. `marie1-covar` [ER]

We also must choose an ϵ . A large ϵ means that the regularization will be strong (we will be smoothing more) and a small ϵ means the regularization is not strong (we honor the model more). For now, we are trying to choose an ϵ that is somewhere in the middle, so that our result is slightly smoothed. We want to try to fill the null space in a reasonable way.

RESULTS

Elf North Sea dataset

The first dataset we applied this RAD preconditioned inversion to was an Elf North Sea dataset. It is a 2-D synthetic created based on a real 3-D survey. Its velocity model can be seen in Figure 4. This dataset is known to have illumination problems under the edge of the salt (Prucha et al., 1998). We first created CIGs by just RAD migration, then we created CIGs by preconditioned inversion. The inversion results are from just one iteration.

Figure 5 shows a comparison of the results from a CMP location that is in a simple area of the subsurface. Note that the inversion result is cleaner, smoother, and more continuous than the migrated result. A good example is the event at 4400 meters, which has been cleaned up and now covers almost twice as many reflection angles as it did in the migrated result while still being reasonable.

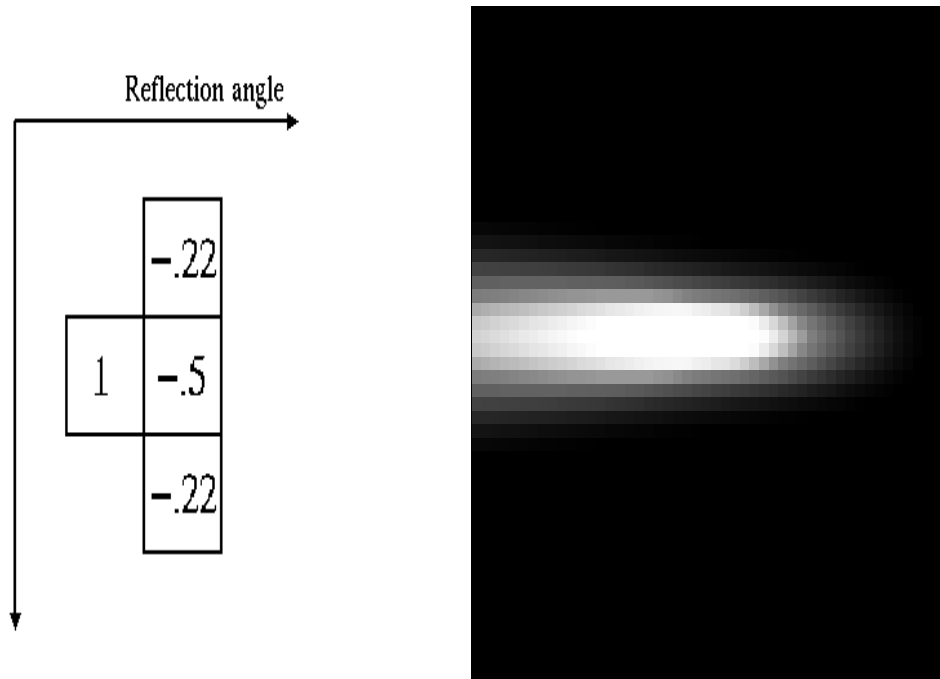


Figure 3: Left: steering filter used for regularization. Right: impulse response of steering filter. `marie1-filtres` [NR]

Figure 6 displays the CIGs for a CMP at the edge of the salt. Once again the inversion result is better than the migrated result, and even the event for the poorly illuminated reflector at depth 4400 meters is more continuous.

BP multiple dataset

We also applied this method to a synthetic multiple dataset provided to us by BP. This is a complicated dataset designed to have extremely nasty multiples. Its velocity model is in Figure 7. Once again, we can expect illumination problems under the edges of the salt body (Muerdter et al., 1996). Even after only one iteration, the RAD preconditioned inversion has produced CIGs that are cleaner and more continuous than RAD migration.

Figure 8 displays a CIG taken from a point away from the salt body. The migrated result has good, continuous reflectors, but there are artifacts between 6 kilofeet and 10 kilofeet and there is a multiple at depth 11.5 kilofeet. The inversion result cleans these artifacts up and attenuates the multiple.

Figure 9 shows a CIG taken at the right edge of the salt body. There are many artifacts and multiples in both the migrated and the inversion results, but the strength of the artifacts and the multiples is reduced in the preconditioned result. Preconditioning has also made the event from the reflector below the salt at depth 13 kilofeet more continuous.

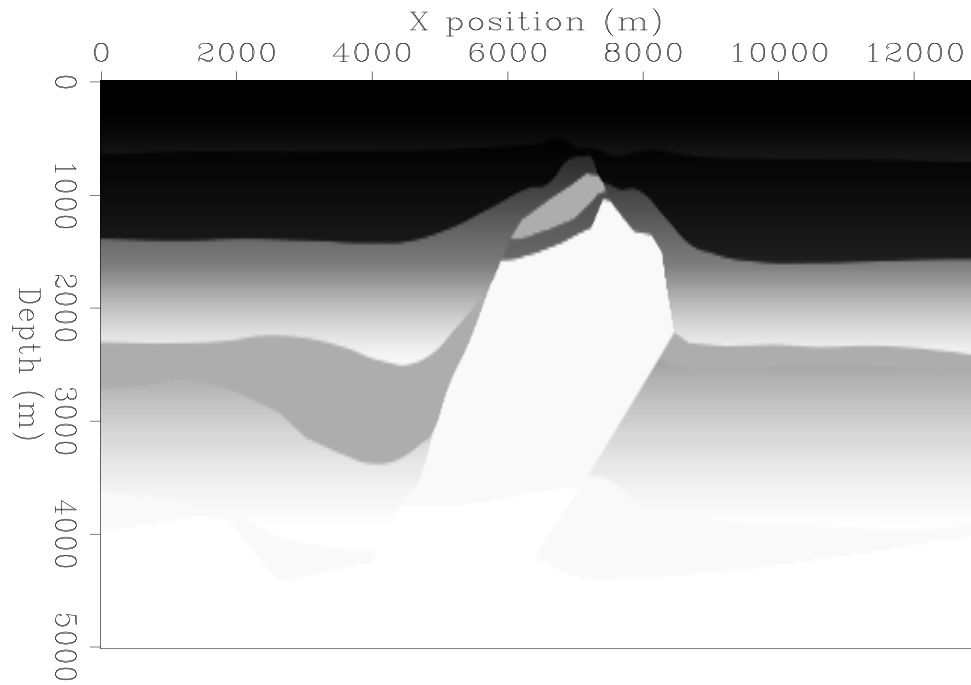


Figure 4: Velocity model of the Elf North Sea dataset. `marie1-elfvel` [ER]

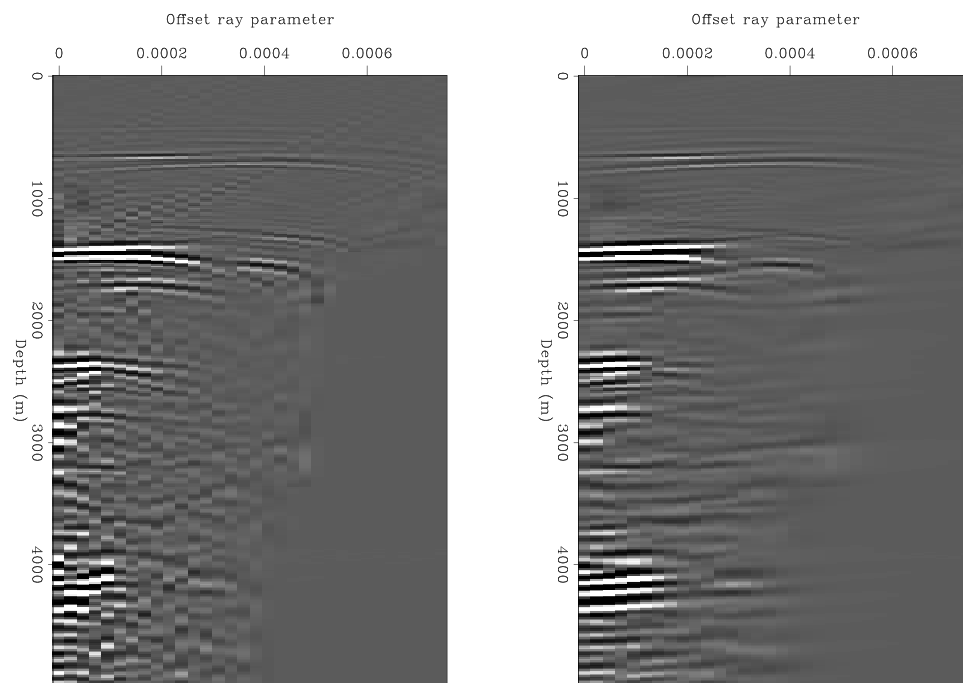


Figure 5: Left: RAD CIG from migration only at CMP 200. Right: RAD CIG from inversion at CMP 200. `marie1-elf.comp200` [CR]

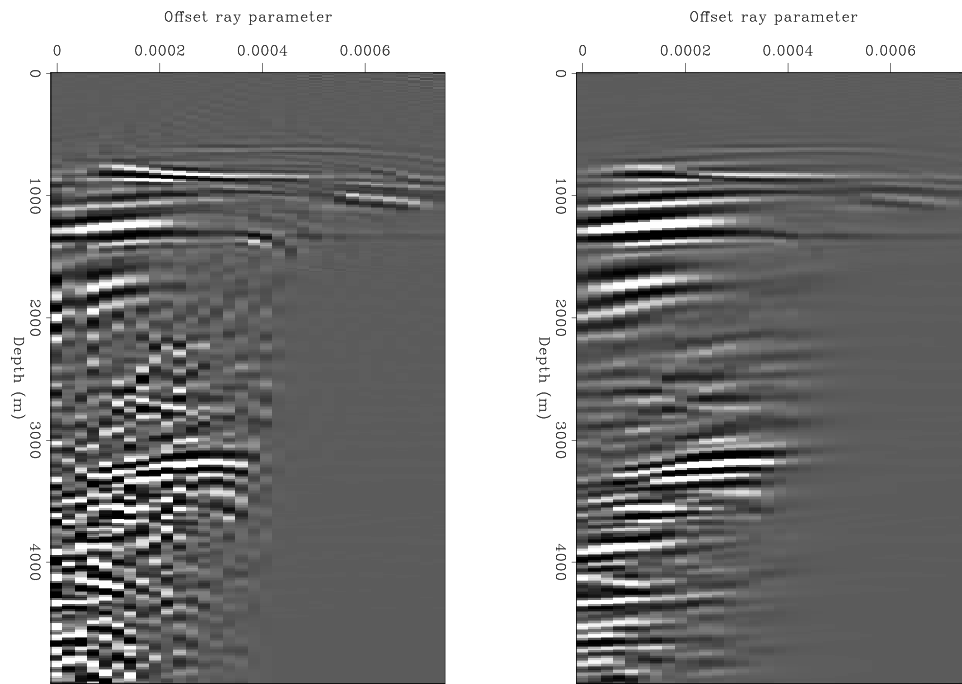


Figure 6: Left: RAD CIG from migration only at CMP 7300. Right: RAD CIG from inversion at CMP 7300. marie1-elf.comp7300 [CR]

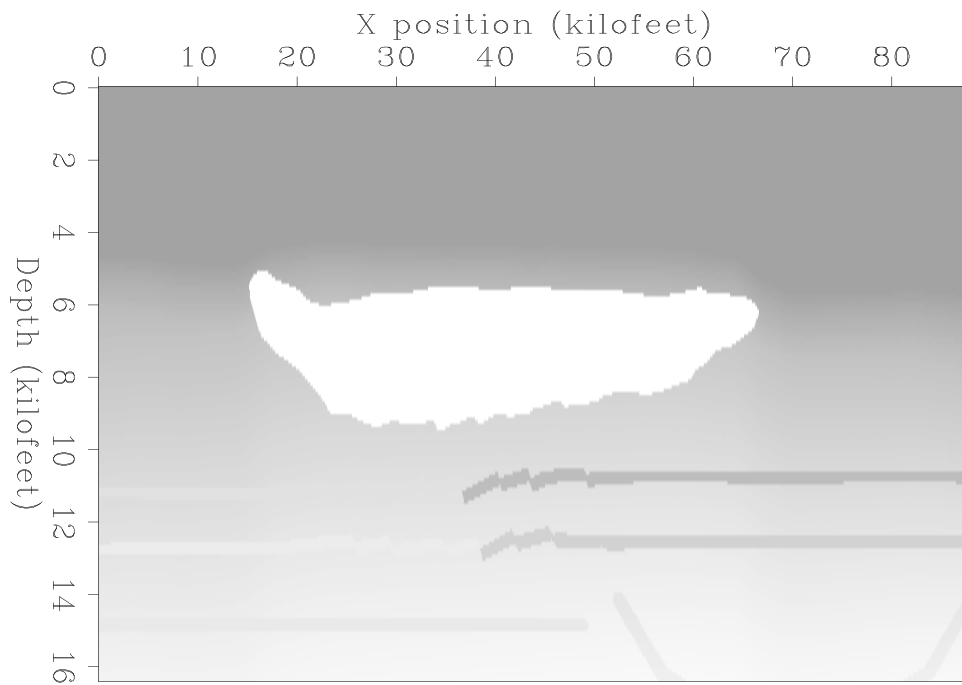


Figure 7: P-wave velocity model of the BP multiple dataset. marie1-bpvel [ER]

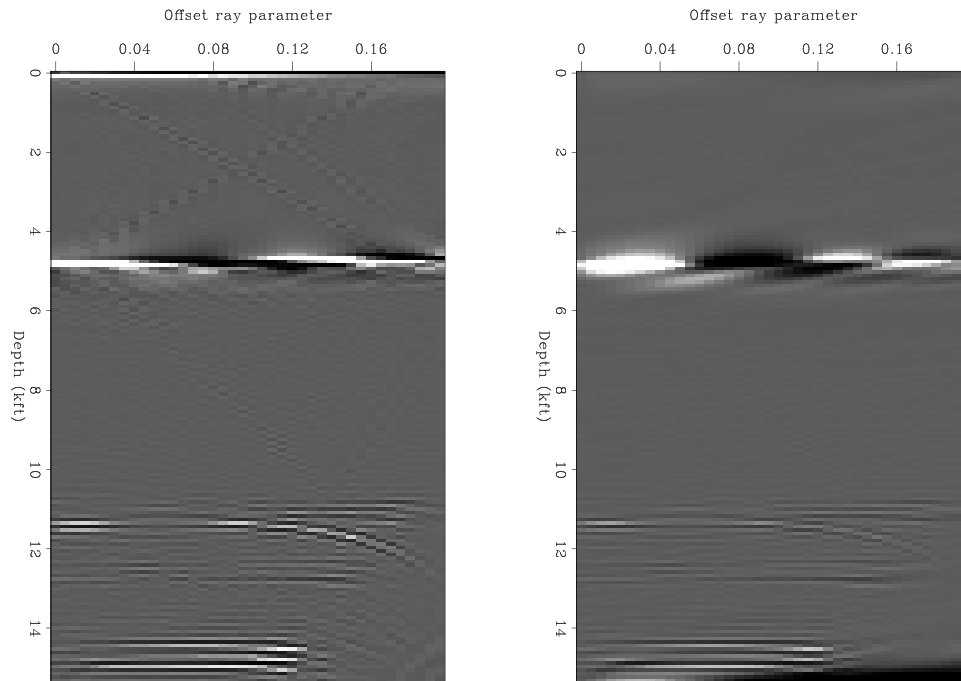


Figure 8: Left: RAD CIG from migration only at CMP 10. Right: RAD CIG from inversion at CMP 10. `marie1-BP.comp10` [CR]

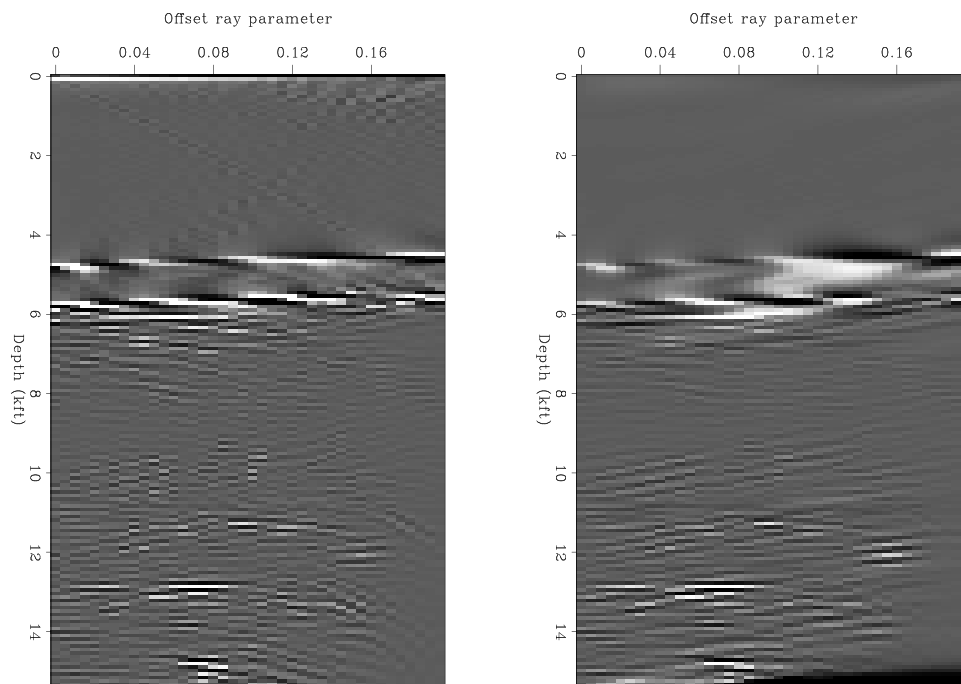


Figure 9: Left: RAD CIG from migration only at CMP 66.33. Right: RAD CIG from inversion at CMP 66.33. `marie1-BP.comp66.33` [CR]

CONCLUSIONS

Regularization in the reflection angle domain helps clean up the artifacts in the common image gathers and improves the continuity of the events in the CIGs. The use of steering filters as our regularization operator is a simple and effective choice. The additional cost of inversion is worthwhile in complex areas.

ACKNOWLEDGMENTS

We would like to thank Elf and IFP for the Elf North Sea synthetic dataset and BP-Amoco for the BP multiple dataset.

REFERENCES

- Chemingui, N., 1999, Imaging irregularly sampled 3D prestacked data: Ph.D. thesis, Stanford University.
- Claerbout, J. F., 1991, Design of inverse Kirchhoff-style filters by LSCG: SEP-72, 33–38.
- Claerbout, J., 1998, Multidimensional recursive filters via a helix: *Geophysics*, **63**, no. 05, 1532–1541.
- Clapp, R. G., Fomel, S., and Claerbout, J., 1997, Solution steering with space-variant filters: SEP-95, 27–42.
- Duquet, B., and Marfurt, K. J., 1999, Filtering coherent noise during prestack depth migration: *Geophysics*, **64**, no. 4, 1054–1066.
- Fomel, S., Clapp, R., and Claerbout, J., 1997, Missing data interpolation by recursive filter preconditioning: SEP-95, 15–25.
- Fomel, S., 1997, On model-space and data-space regularization: A tutorial: SEP-94, 141–164.
- Harlan, W. S., 1986, Signal-noise separation and seismic inversion: SEP-47.
- Muerdter, D. R., Lindsay, R. O., and Ratcliff, D. W., 1996, Imaging under the edges of salt sheets: a raytracing study: 66th Annual Internat. Mtg., Soc. Expl. Geophys., Expanded Abstracts, 578–580.
- Nemeth, T., Wu, C., and Schuster, G. T., 1999, Least-squares migration of incomplete reflection data: *Geophysics*, **64**, no. 1, 208–221.
- Prucha, M. L., Clapp, R. G., and Biondi, B. L., 1998, Imaging under the edges of salt bodies: Analysis of an Elf North Sea dataset: SEP-97, 35–44.

Prucha, M., Biondi, B., and Symes, W., 1999, Angle-domain common image gathers by wave-equation migration: 69th Ann. Internat. Meeting, Soc. Expl. Geophysics, Expanded Abstracts, 824–827.

Richter, C. F., 1941, *Elementary Seismology*: Freeman, San Francisco.

Sava, P., and Fomel, S., 2000, Angle-gathers by Fourier Transform: SEP-**103**, 119–130.

Tarantola, A., 1986, A strategy for nonlinear elastic inversion of seismic reflection data: *Geophysics*, **51**, no. 10, 1893–1903.

ten Kroode, A. P. E., Smit, D.-J., and Verdel, A. R., 1999, Linearized inverse scattering in the presence of caustics: *Wave Motion*.

Xu, S., Chauris, H., Lambare, G., and Noble, M., 1998, Common angle image gather - a strategy for imaging complex media: Summer Research Workshop: Depth Imaging of Reservoir Attributes, EAGE-SEG, Expanded Abstracts, X012.

